Scientia Iranica A (2015) 22(3), 699–708

SCIENTIA IRANICA

Sharif University of Technology
Scientia Iranica
Transactions A: Civil Engineering
www.scientiairanica.com

Shear-torsion interaction of RC beams strengthened with FRP sheets

S.B. Talaeitaba* **and D. Mostofinejad**

Department of Civil Engineering, Isfahan University of Technology, Isfahan, P.O. Box 8415683111, Iran.

Received 16 January 2014; received in revised form 20 July 2014; accepted 22 September 2014

KEYWORDS
Interaction curve;
Reinforced concrete beams;
Combined shear-torsion;
FRP sheets;
Strengthening.

Abstract. One of the most common options for structural strengthening and rehabilitation is the use of FRP sheets for shear-torsion strengthening of Reinforced Concrete Beams (RCBs). Their widespread use owes much to their ease of application in addition to many other advantages. The availability of technical references and construction codes today makes it easy to calculate the shear and torsion capacities of strengthened beams. Practically, however, it is combined shear and torsion rather than pure torsion that develops in beams. The present article investigates the use of FRP sheets in strengthening RC beams. For the purposes of this study, 14 RC beams were used that were classified into three different sets: one set consisted of 5 non-strengthened (plain) beams and two sets (one with 5 and the other with 4 beams) consisted of RC beams strengthened with CFRP sheets in two different strengthening patterns. The shear-torsion interaction curves were derived for them by loading the beams under a variety of eccentricities ranging from 0 (pure shear) to infinity (pure torsion). The supports were constructed with flexure and torsion rigidity. Laboratory tests revealed that the shear-torsion interaction curves for all the three sets of beams were close to straight lines.

© 2015 Sharif University of Technology. All rights reserved.

1. Introduction

It is now more than two decades since the use of FRP composites became widely accepted for strengthening reinforced concrete members. One of their important applications is in the shear and torsion strengthening of RC beams. Numerous studies have been devoted to the effects of FRP sheets on shear and torsion capacities of concrete members. Pure torsion is practically less common in members; rather, what is observed in most situations is the combined shear and torsion that develops simultaneously. Although it is necessary to calculate the resistance of FRP strengthened beams, to date only limited studies have been conducted in this area [1].

In the 1970's, researchers concentrated their efforts on investigating the behavior of RCBs under combined shear and torsion. Klus was the first to conduct such studies [2]. He studied 10 RCB specimens under combined shear and torsion, and the curve he derived for shear-torsion interaction was bilinear. In this curve, the longitude represented the shear strength and the intercept was the torsion strength. At a point on this curve where the ratio of the current shear to maximum shear strength equals 0.6, a shift occurred in the incline. Klus also reported other interaction curves derived by other researchers of his time. Among these curves were a circular one and a linear one, the latter changing its direction near both horizontal and vertical axes to become perpendicular to them.

Between 1970 and 1978, other researchers, including Zia [3], Elfern et al. [4], and llos and Martin [5], studied concrete beam behavior under combined shear, torsion, and flexure. Their investigations were based on

*. *Corresponding author. Tel.: +98 31 33912700;*
Fax: +98 31 33912701
E-mail addresses: talaeetaba@iaukhsh.ac.ir (S.B. Talaeitaba); dmostofi@cc.iut.ac.ir (D. Mostofinejad)

theoretical analysis of fracture mechanics. They found that the curves tended to be quadratic at high flexure to torsion ratios but linear at low ratios. Mirza also claimed that web stirrups would affect RCB behavior under shear and torsion, so that the linear curve would change into a circular quadrant when the amount of these stirrups increased [6].

Further analytical and theoretical investigations were conducted on the behavior of concrete beams under combined shear and torsion. In 1993, Rahal studied such beams and solved the relevant equations using the modified compression field theory [7]. He derived linear interaction curves for some of the beams, tested under different eccentricities. Taweep et al. (2003) investigated the behavior of four RCB specimens exposed to both shear and torsion [8]. They also obtained a liner relationship between shear and torsion strengths. Bairan and Bernat (2007) exploited the fundamental assumptions of materials mechanics to derive differential equations for beam behavior under simultaneous torsion and shear, and used numerical methods to solve the equations [9].

Strengthened beams under combined shear and torsion were first studied by Deifalla and Ghobarah in 2010 [10]. In their study, they tested six half-scale T-shaped beams. From among these, two were used as control and four were strengthened for the experiment. The strengthened beams were loaded under just one eccentricity (the ratio of torsion to shear ($e = T/V$)) for which evidently no interaction curves could be plotted. These researchers also derived an analytical algorithm based on the compression field theory which could also be used to study beams under combined shear and torsion. However, to the best of our knowledge, no study seems to have been reported in the literature on FRP-strengthened beams under combined shear and torsion. Knowledge about this behavior becomes significant in designing reinforced concrete members strengthened with FRP sheets and subjected to both shear and torsion. There are presently equations presented in codes such as ACI440 or fib CEB-FIP for determining the shear resistance of such beams [11,12]. While research efforts still continue in this area, there are only a few codes which provide relations for calculating torsion resistance in strengthened beams. In doing so, these relations use a combination of concrete, stirrup, and FRP capacities, similar to the case with shear resistance calculations [12,13]. Recent investigations, however, have indicated the inadequacy of this method. Deifalla and Ghobarah, for instance, carried out a comprehensive comparison of calculation results obtained from lab-scale experiments and those obtained from the fib code to show that the average capacity obtained by the fib code only accounted for around 30% of the laboratory results [14]. Moreover, no mention is made in recent codes of the combined shear-torsion strength of FRP strengthened beams.

The main objective of the present study is to derive the shear-torsion curves for FRP-strengthened RCBs. For this purpose, 14 specimens were made, 5 of which were used as control without any strengthening FRP sheets. The control specimens were subjected to loading under 5 different eccentricities, and the shear-torsion interaction curves were plotted for them. The rest of the beams were grouped into two series: one comprising 4, and the other, 5 beams, all of which were strengthened with FRP sheets, but in two different patterns. Every individual beam was then subjected to loading under different eccentricities and the shear-torsion interaction curves were derived from the results. Below is a description of beam specifications, the strengthening sheets and patterns used, the test process, and the results obtained.

2. Research significance

As mentioned, equations and guidelines are currently available for calculating shear and torsion capacities in strengthened beams. Once interaction curves become available for such beams, it will be possible to determine pure shear and torsion capacities for the strengthened sections of RC members subjected to simultaneous shear and torsion. The strengthening design adequacy can then be evaluated using the interaction curve thus obtained for the demanded shear and torsion.

3. Experimental procedure

As already pointed out in the introduction, the objective of the present study is two-fold: To investigate the shear and torsion behavior of FRP-strengthened RCBs, and to derive their shear-torsion interaction curves. To reduce the effect of flexural moment in the specimens subjected to simultaneous shear and torsion, an area of the beam that experiences a slight flexural moment, but fixed shear and torsion is required. In previous studies, such as Rahal [7], this area was created using multi-span beams, in which shear and torsion forces, but a slight flexure, existed midway at the middle span. These conditions can also be created, albeit for only one eccentricity, by applying eccentric point loads and creating supports at the two ends of the beam [1]. (It must be noted that it is not possible to test the beam at every arbitrary eccentric point unless the setup, or the load carrier, is changed for each eccentricity.)

Considering the special conditions of the loading equipment, fixed supports were used in the current study. In this test system, the supports were designed to restrain flexural and torsional rotations, while loading was applied at the middle with or without

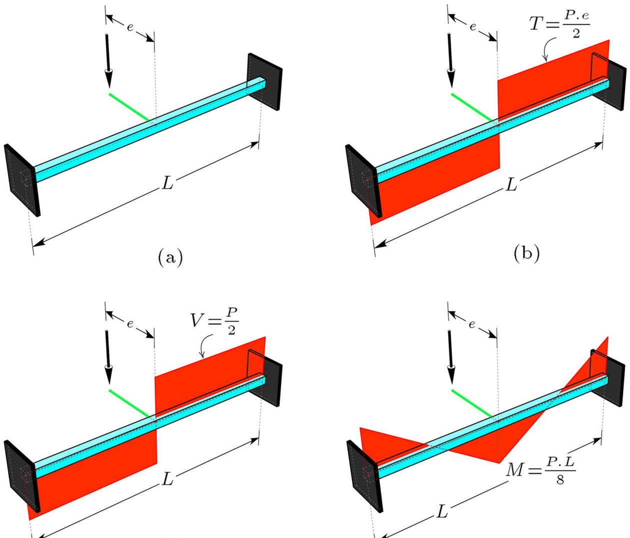

Figure 1. Loading and internal forces in the test beams: (a) Loading scheme; (b) torsion diagram; (c) shear force diagram; and (d) flexural moment diagram.

eccentricity (pure shear). Figure 1 shows the schematic view of the internal forces in the beam. In this case, an area with a slight flexural moment, but with fixed shear and torsion, was created within one fourth of the beam length from each end (from each support); any section in this area could be used for the test.

4. Test set up

To maintain the flexural rigidity at the ends, two H-shaped decks were used on the top and bottom of the beam. They were coupled together using a stiffener on one side and bolts that were tightened after the installation of the beam on the other (Figure 2(a)). Also, the spaces between the beam and the decks were filled with grout so that no differential rotations would occur.

To accomplish torsion rigidity, as shown in Figure 2(b), two stiffened L-shaped elements were tightened to the H-shaped decks and their gaps with beam sides were filled with grout to resist any torsion rotation. The length of these H-shaped elements was long, so that the beam could rest at each section along its length. The loading actuator was fixed, such that eccentricity could be created wherever the beam rested. If the beam was located exactly under the loading actuator, then a situation of pure shear would obtain; otherwise, either a situation of simultaneous shear-torsion or one of pure torsion would be created.

To test the beams under pure torsion, a shear compensator was placed in the middle as a support in order to prevent the development of shear and flexure in the beam. This support, shown in Figure 3, would absorb the whole shear load. Prior to grouting, two foam pieces were placed at each end between the beam sides and the grout to make sure that this part would perform well. In this way, the vertical rigidity of the support would be almost zero and the vertical load (shear load) would be transferred to a hinged member all along.

Also, some deflection gages were used to ensure the workability of the system. The support rotation was then calculated by dividing the difference between the two readings at the two gages placed

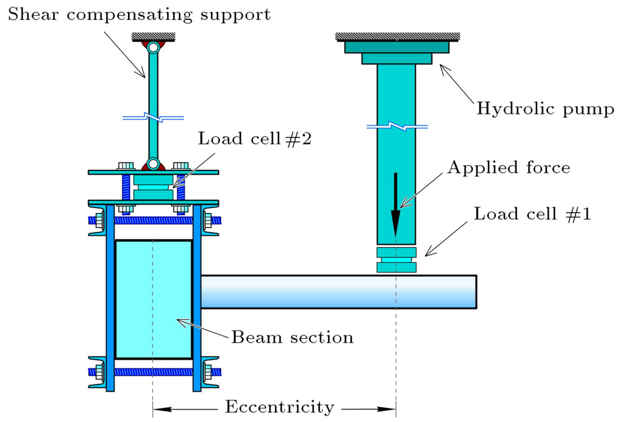

Figure 3. Schematic view of loading system for pure torsion test.

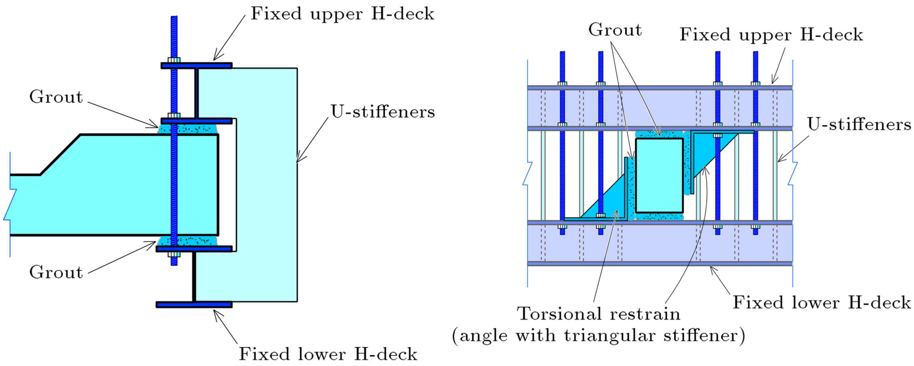

Figure 2. Detail of test beam supports: (a) Side view (flexural fixity); and (b) end view (torsional fixity).

along the support, by their distance. The results were examined in several cases to ensure adequate flexural rigidity on both sides of the supports. Also, deflection gages were installed on both sides of the beam to measure horizontal displacement, from which torsion rotation could be obtained. The results in this case also showed adequate torsion rigidity of the supports. References [15,16] provide a detailed description of the methods to ensure adequate support performance and proper loading procedures.

For the pure torsion test, a load cell was placed under the hinged vertical member (Figure 3). This load cell was to ensure that the load applied to the vertical member is equal to the eccentric load exerted on the beam (the load reading on load cell # 1 in Figure 3), and that no shear or flexure is thereby created in the beam under pure torsion. Finally, a portable metal belt, 250 mm in length, was also used in the middle of the beam to help its eccentric loading (Figure 3).

Figure 4(a) which shows a beam under pure torsion, and Figure 4(b) which shows a beam under combined shear and torsion, depict the difference between the two pure torsion and combined shear and torsion tests. It is seen in Figure 4(a) that the hinged member compensating the shear force is connected to the top part of the metal belt around the beam.

5. Experimental specimens

Considering the invented setup and the distribution of the internal forces in the beam, the areas to be tested lie at a quarter of the beam's length from each end. To run the tests, beams were constructed as shown in Figure 5. At the inclination point of the bending moment, the beam's depth and the stirrups were reduced in order to direct the shear-torsion failure of the beam toward this area. In addition, the depth and the stirrups around areas with higher bending moments were increased to avoid any flexural or shear-torsion failures in these areas. With the special specimens thus prepared and given, the beam sections at the beams stronger areas are adequately resistant against bending or shear-torsion moments. It can be expected that the behavior observed in the specimens under testing is compatible with that of the weakened sections; in other words, beam failure occurs at the weakened section of

(a) (b) (c)

Figure 4. Beam specimens under test: (a) Pure torsion: (b) combined shear-torsion; and (c) 2 foam pieces for pure torsion test.

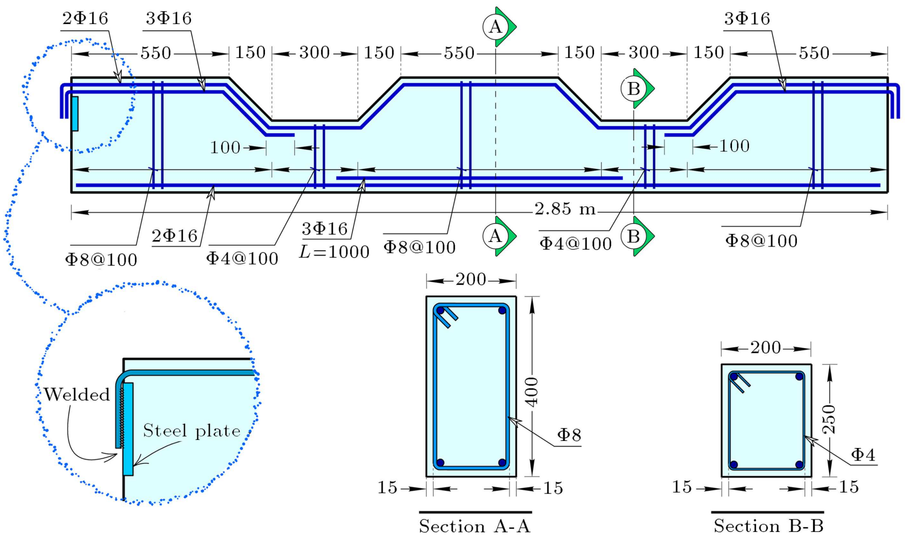

Figure 5. Test beam details (dimensions in mm).

Table 1. Test specimens and loading eccentricity.

Concrete mix. seri.	No.	Specimens name	Eccentricity (mm)
$E(f'_c = 34.9$ MPa)	1	E0	$e = 0$
	2	E1	$e = 290$
	3	E2	$e = 470$
	4	E3	$e = 616$
	5	E4	$e \approx \infty$
$A(f'_c = 28.4$ MPa)	6	A0	$e = 0$
	7	A1	$e = 290$
	8	A2	$e = 470$
	9	A3	$e = 616$
	10	A4	$e \approx \theta$
$B(f'_c = 35.4$ MPa)	11	B0	$e = 0$
	12	B1	$e = 470$
	13	B2	$e = 616$
	14	B4	$e \approx \infty$

the beam, while other sections only serve to transfer loads.

The longitudinal bars and stirrups used for these tests were 16 mm and 8 mm in diameter, respectively, with yield strength of 400 Mpa. In the test region, stirrups were reduced to 4 mm in diameter and 240 MPa in yield strength.

To ensure adequate anchorage of the upper reinforcement, mechanical anchorage was employed that consisted of an 8-mm steel plate placed inside the mold prior to concrete casting, and welded to the upper bars of the beam.

A total number of 14 beams with different batch mixes were used in this study. Table 1 presents the labels for each set of specimens, along with the concrete compressive strengths measured on the day the test was run. To derive the shear-torsion interaction curves for each set of specimens, identical specimens were made, and each specimen was tested under a specified eccentricity. The eccentricities are also presented in Table 1. A value of "zero" for eccentricity means testing under pure shear, while "infinity" represents testing under pure torsion. In other words, infinite eccentricity in the case of E4, A4, and B4 specimens means that these specimens were subjected to pure torsion, although they were practically tested under an eccentric load of 470 mm. However, given the hinged vertical member and the use of foam pieces described above, shear force could claim to be negligible and the specimens were actually tested under pure torsion.

It must be noted that the specimens labeled "E" lacked any strengthening. The "A" series were strengthened by bonding one layer of CFRP sheets 20 mm in width and a center-to-center spacing of 90 mm. The "B" series were strengthened with sheets 40 mm wide and a center-to-center spacing of 85 mm. The compressive strength of the concrete used was measured at the time of testing using cylindrical samples and represented as f'_c in Table 1.

6. Test observations

During the test, the eccentric loads shown in Table 1 were applied to each specimen. As already mentioned, the test region lying around the inclination point had a section weaker in shear and torsion. In what follows, the observations are described that were made during the loading process accomplished through displacement control.

6.1. Crack initiation and propagation

The first outcome that deserves investigation is the shape of the cracks created in the specimens. To gain a better understanding of the cracking mechanism, each face of the beam being tested was numbered, as shown in Figure 6. It was observed that the first face to crack in all specimens (both strengthened and non-strengthened) was face number two, which is the larger face of the beam which, following the principles of solid mechanics in members under torsion, experiences the greatest shear stress.

As desirably expected, cracks would initiate in the thinned area of the beam and would propagate at an angle of 34 to 40 degrees relative to the beam's longitudinal axis in the control specimens, and at an angle of around 45 degrees in those strengthened. Concurrent with this crack, cracks also appeared in face 4 of both sets of beams under pure shear, and both cracks on face 2 and 4 would then join in the form of a straight line on face number 3. This cracking pattern has also been reported in the relevant references [17]. In the specimens subjected to combined shear and torsion, the cracks initiated on face 2, and continued downward the section (to face 3) to join on faces 1 and 4 after the applied load was increased. The only difference in the cracking in the strengthened specimens was the

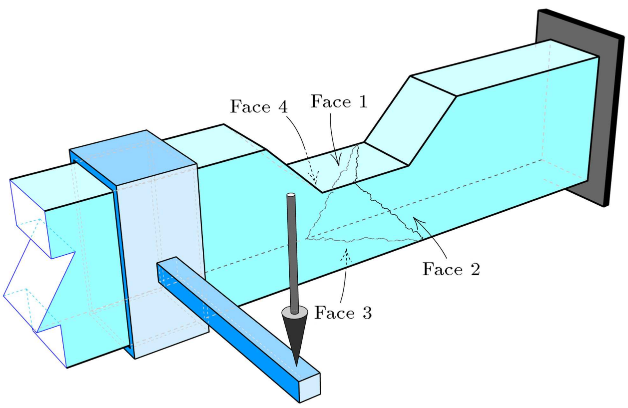

Figure 6. Numbering of beam faces and cracking pattern in pure torsion test.

angle of cracking on different faces in proportion to the different shear-torsion moments, such that the crack angles relative to the beam's longitudinal axis would increase on faces 1 and 3, proportional to the eccentric load applied, but would decrease on faces 2 and 3. The reason for this might be the change in the beam section's behavior from one of pure torsion to one of combined shear-torsion. In this situation, the crack pattern changed from spiral-like cracks, with a closed variable angle that depends on the degree of torsion and the conditions of the section, to diametrical cracks, since the axis of the major stresses created in the beam in an element close to the external side of the beam section draws closer to 45 degrees.

The same cracking sequence and patterning was observed in specimens under pure torsion, while the same spiral-like cracks reported elsewhere were also observed [18]. Figure 7 shows the cracks created in specimens E4, A4, and B4 under pure torsion as examples of the cracking pattern observed.

It is worth mentioning that failure in the control beams occurred at the location of the initial first or second cracks, such that increasing the load after the development of the first crack mostly resulted in the widening of the same crack rather than in the development of new cracks in other faces; in fact, less than three cracks developed, if any. In the specimens in series "*A*" in which external strengthening was lower than that in series "*B*", the situation was slightly different. As seen in Figure 6, a few more cracks were developed in other faces. This is while more cracks developed after the first crack in series "*B*" specimens, which enjoyed a stronger external strengthening. Also, the crack in series "B" developed within the area between the FRP sheets in the concrete section propagated under the FRP sheets toward other faces. Finally, no cracks of any type, due to either bending or shear-torsion moments, were observed in the stronger regions of the beam. This beam behavior was quite expected, as we had hypothesized that it must be possible to investigate the behavior of a strengthened section in the weakened beam area

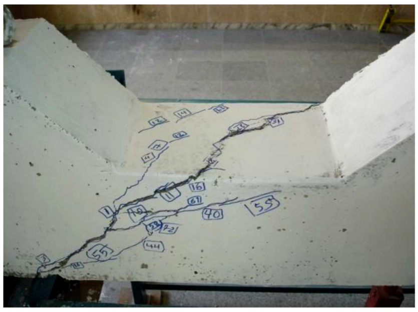

E4 (faces 1 & 2-left side)

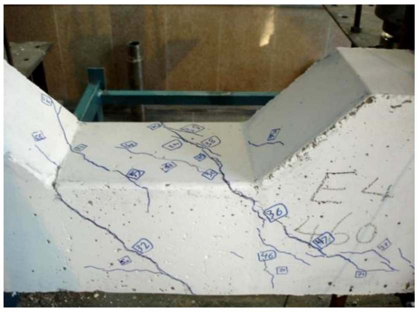

E4 (faces 1 & 4-right side)

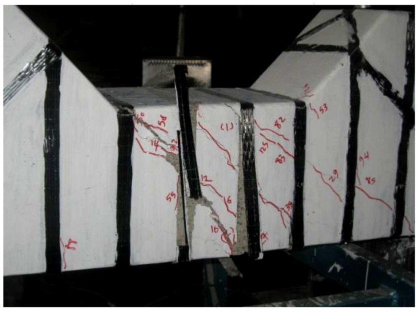

A4 (faces 1 & 2)

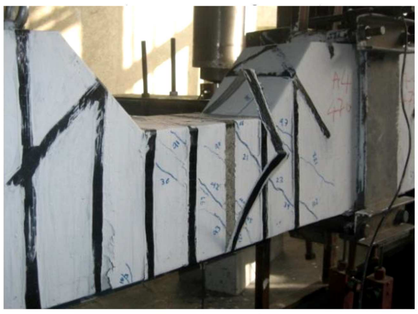

A4 (face 4)

B4 (faces 1 & 2)

B4 (faces 1 & 4)

Figure 7. Crack pattern in specimens under pure torsion.

by changing the beam shape to the one described above.

6.2. Crack width

The tests revealed that cracks in the strengthened specimens were far narrower than those in the non-strengthened specimens, so that a reduction of 20% was observed in crack width compared to that in the control specimen. This is evidenced by width measurements using magnifiers, indicating average crack widths of 2.5 mm and 2 mm in series "A" and "B", respectively, while the crack width in the control specimen was 10 mm.

Once the cracks had developed, other cracks parallel to the FRP fibers, gradually appeared within the area between FRP sheets and concrete surface (cracks in the resin) as a result of increasing load, which indicated FRP debonding. This was observed in all the strengthened specimens (Figure 8). Continued loading in all the 9 strengthened specimens, however, led to the ultimate debonding of the FRP sheet bonding. The debonding, as seen in Figure 7, generally occurred in areas close to the section corners at a distance of around 200 mm from the corner and in the larger face. It needs to be mentioned that this area is the one characterized by the greatest shear stress (including shear stress due to shear or torsion) which is the major cause of the debonding observed.

6.3. Failure loads

Table 2 presents the cracking and failure loads for each specimen. According to the table, the cracking load increased by about 25% in series "A" and by about 50% in series "B" compared to series "E". Also, the failure load in series "A" and "B" specimens showed increases by around 62% and 97% (almost two times), respectively, compared to series "E". The increases observed in both cracking and failure loads

Figure 8. Start of debonding of FRP laminates.

Table 2. Experimental results.

Specimen	Cracking load (kN)	Ultimate load (kN)	Increase in cracking load (%)	Increase in ultimate load (%)
E0	1.00.0	134.0	—	—
E1	38.0	49.2	—	—
E2	21.0	33.7	—	—
E3	18.0	29.0	—	—
E4	20.0	55.0	—	—
A0	135.0	188.0	35.0	40.3
A1	40.0	77.3	5.3	57.1
A2	24.0	57.2	14.0	69.7
A3	27.0	49.0	50.0	69.0
A4	24.0	95.4	20.0	73.5
B0	133.0	246.0	33.0	83.6
B1	38.0	72.8	80.9	116.0
B2	25.0	57.2	38.9	97.2
B4	30.0	104.4	50.0	89.8

in series "B" specimens compared to those in series "A" are perfectly reasonable and can be justified by the enhanced strengthening in series "B". The increased cracking in the strengthened specimens can be explained by reference to the fact that the greatest shear stress in specimens occurs in the external wall of the beam section where shear-torsion cracks initiate. The bonding of FRP sheets around the section in the strengthened specimens causes the shear stress around the section to transform to tensile stresses in the FRP sheet. Considering the conformity between the strain of the FRP sheet and the concrete surface, the tensile stress thus formed can be rather high due to the high ratio of modulus of elasticity of carbon fibers to that of concrete. Thus, the shear stress within the concrete is reduced (the farthest concrete threads of the section) and, thereby, the concrete cracks at higher loads. This can be clarified by comparing the results for the two series, "A" and "B", reported in Table 1. The $\frac{b_f}{s}$ ratio (width to FRP sheet spacing) is almost equal to 0.2 for series "A" and 0.47 for series "B". The increased value of cracking load for the specimens under pure torsion in the table is almost 2.5 times the lower one (almost equal to the ratio of 0.47 to 0.2) and lies between the two series.

It is also clear from Table 2 that the increased strengthening in the specimens subjected to pure shear (i.e., B0 vs A0) did not lead to the slightest change in their cracking load. This is while the ultimate load in series "B" vs. that in series "E" showed a 100% increase compared to the same increase in series "A" vs. series "B" (i.e. 83.4% vs. 40.3%).

The effects of strengthening were totally different in the specimens under pure torsion. In the beam B4, the cracking load and the failure load increased by 50% and 90%, respectively, whereas these values for beam A4 were 20% and 73%, respectively. This means that increased strengthening in the specimens under pure torsion has a considerable effect on the failure load of the specimen. In the specimens under pure torsion, however, both loads increased with increasing strengthening.

Compared to the control specimens, in the other specimens in series "A" subjected to combined shear and torsion, both failure and cracking loads increased with increasing eccentricity.

7. Shear-torsion interaction curves

The major objective behind this study was to determine the relationship between the shear force and the torsion moment and to extract their interaction curve. The torsion moment at the time of section failure was obtained by multiplying the values for loading by the eccentricity value for each specimen and dividing the product by two. Based on the beam shape, the changes made in the section and its reinforcement at the point of failure (i.e., around the bending incline), and the provisions explained above about the specifications of the specimens, we hypothesized that the shear-torsion failure must occur at the weakened section of the beam; this was realized in practice. Thus, it may be admitted that the calculated values for shear force and torsion moment at the time of failure can be considered as the simultaneous shear-torsion capacity of the smaller section shown in Figure 4.

Based on the values obtained for the shear force and torsion moment at the time of failure, the shear-torsion interaction curves in Figure 9 were developed. The dashed curves in this figure are obtained by connecting the test results. The solid line curves represent the regression of the test results for each series of beams. Clearly, the interaction curves are very close to straight lines.

As already mentioned in the introduction, the

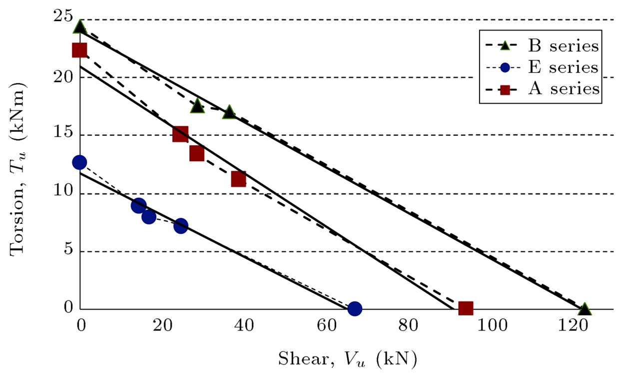

Figure 9. Shear-torsion interaction curves.

interaction curves plotted as straight lines obtained for non-strengthened RCBs are in agreement with those reported in references [2-4,6,7]. It is also interesting to note that in his study, Klus [2] derived the same curve as a straight line for specimens with sections approximately similar to those studied here, but with reinforcement 4 times the minimum shear-torsion reinforcement specified in ACI318-08 [19]. So, comparison of the results obtained from the present study and those from other investigations indicates that the curve obtained here applies to non-strengthened RC beams.

The curves derived for FRP-strengthened specimens can be compared with those obtained for beams with a high amount of stirrup. Thus, the curve will be almost linear, as also reported by Klus.

A variety of methods have been proposed in the literature for deriving the shear-torsion interaction curves for RC beams; these include:

1. Skew bending method;
2. MCFT (Modified Compression Field Theory);
3. Nonlinear finite element analysis;
4. Experimental tests.

These different methods yield different interaction curves [2-4,6,7,20,21]. However, most of them indicate that the interaction curves are either linear or bilinear, or that they are almost circular for over-reinforced members because of the concrete cover spalling. In the recent case, the interaction curve reportedly tends to be perpendicular to the axis of torsion (i.e., the vertical axis) for a shear force value near zero (pure torsion). However, some references report a linear interaction curve (or fit the line to the interaction curve) for all the different cases.

In the present study, the results are in agreement with those reported in the literature for two reasons: 1) The amount of torsional reinforcement (which is minimal); and 2) There was no cover spalling due to the high performance of FRP torsional strengthening, almost up to ultimate load. It was also noted in this manuscript that Klus reported a linear curve for specimens with torsional reinforcement up to 4 times the minimum recommended by the relevant code, and, as can be seen in Table 2, that the maximum load in our specimens increased by about 116%, which can be about 2 times if both steel and FRP reinforcements are considered.

It may, therefore, be concluded that the interaction curves in the FRP strengthened beams (if FRP stirrups are closed (□) and not open (U or ...)) are linear or semi-linear for two reasons: 1) There is almost no spalling, and 2) The FRP sheets mainly exhibit a linear behavior.

Based on the linear interaction curve derived in this paper and designating the shear and torsion capacities of the strengthened beam under pure shear and torsion as V_{u0} and T_{u0}, and the combined shear and torsion capacity as V_u and T_u, the following equation will represent the relation between V_u and T_u:

$$\frac{V_u}{V_{u0}} = 1 - \frac{T_u}{T_{u0}}. \tag{1}$$

8. Summary and conclusions

To derive the shear-torsion interaction curve for CFRP-strengthened beams, 14 specimens were made which consisted of 9 strengthened with CFRP sheets in two different patterns and 5 used as control. The beams were subjected to eccentric loads in the laboratory. Using the invented setup and the loading system, it was possible to test the specimens under pure shear, pure torsion, and combined shear and torsion, using a hydraulic jack. The following results were obtained:

1. Using FRP stirrups resulted in an increased cracking load of 5 to 81%. The least increase was observed when the specimen was strengthened with FRP sheets 20 mm wide, spaced 90 mm apart, and to an eccentric load of 290 mm. The highest increase was observed in specimens bonded with 40-mm FRP sheets, spaced at 85 mm, and loaded under 470 mm of eccentricity. The increase in failure load was around 40 to 116%.
2. Under combined shear and torsion, the specimens with lower strengthening showed a higher increase in cracking load, as a result of increasing eccentricity, than the control beams. Under the same conditions, specimens with higher strengthening acted diversely but the same pattern was observed for the failure loads.
3. Compared to the control, more cracks appeared in strengthened specimens all around the test region, and the cracks were more easily detectable in specimens with greater strengthening.
4. The crack width in strengthened specimens was limited to 20% of that in the control specimens.
5. The shear-torsion interaction curves plotted for the three series of specimens were very close to straight lines. Based on the results obtained, Eq. (1) was developed to express the shear-torsion relationship in FRP-strengthened sections.

References

1. Deifalla, A. "Behavior and strengthening of RC T-girders in torsion and shear", PhD Thesis, McMaster University (2007).
2. Klus, J.P. "Concrete beams under combined torsion and shear", *ACI Journal*, pp. 210-216 (March 1968).
3. Zia, P. "What do we know about torsion in concrete members?", *Journal of the Structural Division*, **96**, pp. 1185-1199 (June 1970).
4. Elfern, Lennart, Karlsson, Inge and Losberg, Anders, "Torsion-bending-shear interaction for concrete beams", *Journal of the Structural Division*, **100**, pp. 1657-1676 (August 1974).
5. Allos, Atheel E. and Martin, L.H. "Plain concrete tee beams subject to torsion, bending and shear", *Building and Environment*, **13**, pp. 125-134 (1978).
6. Mirza, M.S. "Ultimate strength of reinforced concrete beams in combined torsion and shear", *Journal of the American Concrete Institute*, **65**(9), pp. 788-790 (Sept. 1968).
7. Rahal, K.N. "The behavior of reinforced concrete beams subjected to combined shear and torsion", PhD Thesis, University of Toronto (1993).
8. Taweep, Ch., Suapphong, K. and Chayanin, H. "Experimental investigation on rectangular reinforced concrete beam subjected to Bi-axial shear and torsion", *Songklanakarian Journal of Science and Technology*, **25**(1), pp. 41-52 (2003).
9. Garcia, J.M.B. and Bernat, A.R.M. "Shear-bending-torsion interaction in structural concrete members: A nonlinear coupled sectional approach", *Arch. Comput. Methods Eng.*, **14**, pp. 249-278 (2007).
10. Deifalla, A. and Ghobarah, A. "Full torsional behavior of RC beams wrapped with FRP: Analytical model", *Journal of Composites for Construction, ASCE*, pp. 289-300 (May-June 2010).
11. *Guide for the Design and Construction of Externally Bonded FRP Systems for Strengthening Concrete Structures*, ACI 440.2R-08 (2008).
12. *Externally Bonded FRP Reinforcement for RC Structures, Fib CEB-FIP*, Bulletin14 (July 2001).
13. "User friendly guide for rehabilitation or strengthening of bridge structures using fiber reinforced polymer composites", Report-2002-005-C04, Internet Pdf. File.
14. Deifalla, A. and Ghobarah, A. "Simplified analysis for torsionaly strengthened RC beams using FRP", *Proceedings of the International Symposium on Bond Behaviour of FRP in Structures (BBFS 2005)*, Chen and Teng (Eds.), International Institute for FRP in Construction (2005).
15. Talaeitaba, S.B. and Mostofinejad, D. "Fixed supports in assessment of RC beams' behavior under combined shear and torsion", *International of Applied Science and Technology*, **1**(5), pp. 119-126 (September 2011).
16. Talaeitaba, S.B. and Mostofinejad, D. "A new test setup for experimental test of RC beams under combined shear and torsion", *Advanced Material Research*, **335-336**, pp. 355-358 (2011).
17. Park, R. and Paulay, T., *Reinforced Concrete Structures*, John Wiley & Sons (1974).

18. Ameli, M., Ronagh, H.R. and Dux, P.F. "Behavior of FRP strengthened reinforced concrete beams under torsion", *Journal of Composites for Constructions, ASCE*, pp. 192-200 (March-April 2007).

19. ACI 318-08, Building Code Requirement for Structural Concrete (ACI318M-02) and Commentary-ACI 318R-08, American Concrete Institute, Farming Hills, MI, USA (2002).

20. Ewida, A.A. and McMullan, A.E. "Torsion-shear interaction in reinforced concrete members", *Magazine of Concrete Research*, **23**(115), pp. 113-122 (June 1981).

21. Hasanat, A. and Akhtaruzzaman, A.A. "Beams with small rectangular opening under torsion, bending, and shear", *Journal of Structural Engineering ASCE*, **113**(10), pp. 2253-2270 (1987).

Biographies

Sayed Behzad Talaeitaba is a PhD graduate of Civil Engineering from Isfahan University of Technology, Isfahan, Iran, and Assistant Professor of Azad University, in Iran. His research interests include the mechanical properties of FRP reinforced concrete members and assessment of reinforced concrete structures behavior.

Davood Mostofinejad obtained his PhD degree from Carleton University, Ottawa, Canada, and is currently Professor in the Department of Civil Engineering at Isfahan University of Technology (IUT), Isfahan, Iran. His research interests include analysis and design of RC structures and application of FRP composites in RC structures for strengthening and reinforcement.